

PACS numbers: 42.60.Jf; 42.65.Re
DOI: 10.1070/QE2008v038n04ABEH013717

Features of the formation of a femtosecond Bessel beam by using an axicon

S.N. Kurilkina, A.A. Ryzhevich, S.B. Bushuk, S.V. Solonevich

***Abstract*. The dynamics of the envelope of a pulsed light beam with the transverse field profile described by the Bessel function is studied theoretically and experimentally. The beam is formed by an axicon from a pulse with the Gaussian spatiotemporal envelope. The appearance of a satellite pulse behind the axicon is predicted. The possibility of generating pulsed Bessel light beams with the required diameter and intensity of the central maximum in optical schemes containing an axicon and a lens is shown.**

Keywords: *femtosecond Bessel light beams, axicon.*

1. Introduction

Femtosecond laser pulses providing a high concentration of light energy have found wide applications in the studies of interaction of radiation with matter, investigations of fast processes, and in optical communication systems. An important problem is a strong influence of the frequency dispersion and diffraction divergence on the propagation of ultrashort pulses in a medium. In this connection the so-called dispersion-free and quasi-diffraction-free light fields, in particular, pulsed Bessel light beams (PBLBs) with the transverse field profile described by the Bessel function have attracted recently increasing attention [1 – 4]. Having the intensity maximum on the axis of a beam of diameter of the order of the light wavelength, PBLBs are promising for applications in various optical technologies, including the precision machining of materials, laser cutting and welding, optical diagnostics of technological and biological objects, etc.

Quasi-monochromatic Bessel beams can be obtained by various methods using the Fourier transform of a ring field [5], conic lenses or axicons [6 – 13], holograms [14 – 16], and anisotropic crystals [17 – 19]. One of the most promising methods for generating PBLBs is based on using an axicon. However, the structure of the light field behind an axicon irradiated by an ultrashort pulse has not been investigated in fact so far. The aim of this paper is to study in detail theoretically and experimentally the dynamics of the envelope of a PBLB formed by an axicon from an ultrashort Gaussian pulse.

S.N. Kurilkina, A.A. Ryzhevich, S.B. Bushuk, S.V. Solonevich
B.I. Stepanov Institute of Physics, National Academy of Sciences of Belarus, prosp. Nezavisimosti 68, 220072 Minsk, Belarus;
e-mail: s.kurilkina@ifanbel.bas-net.by, a.ryzhevich@dragon.bas-net.by, s.solonevich@dragon.bas-net.by, s.bushuk@dragon.bas-net.by

Received 6 September 2007; revision received 12 December 2007
Kvantovaya Elektronika **38** (4) 349 – 353 (2008)
Translated by M.N. Sapozhnikov

2. Description of the transformation of Gaussian pulses by an axicon to pulsed Bessel light beams

Consider a light pulse with the Gaussian envelope

$$E(0,\rho,t) = E_0 \exp\left(-\frac{t^2}{t_0^2}\right) \exp\left(-\frac{\rho^2}{2w^2}\right) \exp(\mathrm{i}\omega_0 t), \quad (1)$$

incident on an axicon, where the parameter t_0 is related to the initial pulse FWHM (full width at half-maximum) $\tau_{p0} = (2\ln 2)^{1/2} t_0$; w is the beam half-width at the e^{-1} intensity level; and ω_0 is the central frequency of the pulse. Each of the components of the frequency – time spectrum of the incident pulse (1) propagating through the axicon acquires the phase shift, which linearly depends on the radial coordinate ρ, so that the transmission function of the axicon with a small base angle δ can be written in the form [20]

$$T_{ax}(\rho,\omega) = \exp[-\mathrm{i}\bar{k}\gamma(\omega)\rho], \quad \gamma(\omega) = \delta[n(\omega) - 1], \quad (2)$$

where $\bar{k} = \omega/c$ and $n(\omega)$ is the refractive index of the axicon. One can see from (2) that the transmission function of the axicon depends on the partial wave frequency.

The amplitude distribution $A(r,\omega,z)$ of a field formed by the frequency component of the pulse in a plane perpendicular to the propagation direction z is described by the Fresnel integral [15]

$$\frac{A(r,\omega,z)}{E_0} = -\frac{\mathrm{i}\bar{k}}{z} \exp\left(\mathrm{i}\frac{\bar{k}r^2}{2z}\right) \int_0^R T_{ax}(\rho,\omega) \times \exp\left(-\frac{\rho^2}{2w^2}\right) \exp\left(\mathrm{i}\frac{\bar{k}\rho^2}{2z}\right) J_0\left(\frac{\bar{k}\rho r}{z}\right) \rho \mathrm{d}\rho. \quad (3)$$

Here, R is the axicon radius and J_0 is the zero-order Bessel function. Taking into account the radiation spectrum, we obtain the field amplitude behind the axicon in the form

$$\frac{E(r,z,t)}{E_0} = \frac{1}{2\sqrt{\pi}} \int_{-\infty}^{\infty} t_0 \exp\left(-\frac{\omega^2 t_0^2}{4}\right) \times A(r,\omega,z) \exp\{\mathrm{i}[k_z(\omega)z - \omega t]\} \mathrm{d}\omega, \quad (4)$$

where k_z is the projection of the wave vector on the z axis.

We will analyse expression (4) by using the approximation of $k_z(\omega)$ near the central frequency of the pulse:

$$k_z(\omega) \cong k_{z,0} + k'_{z,0}(\omega - \omega_0) + \frac{k''_{z,0}(\omega - \omega_0)^2}{2} + \frac{k'''_{z,0}(\omega - \omega_0)^3}{6} + \ldots, \quad (5)$$

where $k_{z,0} = \omega_0 \cos\gamma(\omega_0)/c$; $k'_{z,0}$, $k''_{z,0}$ and $k'''_{z,0}$ are the dispersion parameters of the first, second, and third orders, respectively; the prime denotes differentiation with respect to frequency. It follows from (4), taking (5) into account, that the group velocity

$$u = \left(k'_{z,0}\right)^{-1} = \left[\frac{\partial}{\partial\omega}\left(\frac{\omega}{c}\cos\gamma(\omega)\right)\right]^{-1} = \frac{c}{\cos\gamma[1 - \omega\tan\gamma(\partial\gamma/\partial\omega)]} \quad (6)$$

of the pulse formed by the axicon depends not only on the axicon material dispersion (K8 optical glass) but also on its base angle δ (Fig. 1). It follows from (6) that the group velocity of the PBLB exceeds the phase velocity of a Bessel light beam with frequency ω_0.

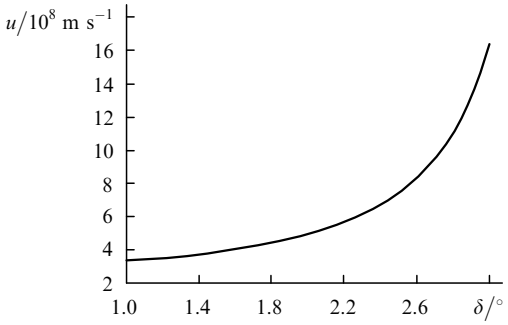

Figure 1. Dependence of the group velocity of the PBLB with the central wavelength 0.85 μm on the base angle δ of the axicon.

By restricting expansion (5) to second-order dispersion terms inclusive and integrating (4), we obtain the analytic expression for the field amplitude behind the axicon

$$\frac{E(r,z,t)}{E_0} = \exp[\mathrm{i}(k_{z,0}z - \omega_0 t)]\left[\frac{A(r,\omega_0,z)}{(1-2\mathrm{i}\mu)^{1/2}} - \frac{4\mathrm{i}\tau\eta}{t_0(1-2\mathrm{i}\mu)^{3/2}} + \frac{\eta_2(1-2\mathrm{i}\mu-2\tau^2)}{t_0^2(1-2\mathrm{i}\mu)^{5/2}}\right]\exp\left(-\frac{\tau^2}{1-2\mathrm{i}\mu}\right), \quad (7)$$

where

$$\mu = \frac{k''_{z,0}z}{t_0^2}; \quad \eta = \left.\frac{\partial A}{\partial\omega}\right|_{\omega_0}; \quad \eta_2 = \left.\frac{\partial^2 A}{\partial\omega^2}\right|_{\omega_0}; \quad \tau = \frac{t - k'_{z,0}z}{t_0}.$$

As follows from (7), due to the frequency dependence of the field amplitude $A(r,\omega,z)$ formed by the partial PBLB wave in a plane perpendicular to the propagation direction z, the radiation intensity $I \sim |E(r,z,t)|^2$ behind the axicon in the distribution minima does not vanish but its value depends on the incident pulse duration.

The use of the second approximation of the dispersion theory is not justified for small values of the parameter $k''_{z,0}$ (in the 'zero-dispersion' spectral regions, where the 'diffraction-free' propagation of light waves occurs) and in the case of femtosecond incident pulses. In this case, the third-order dispersion parameter $k'''_{z,0}$ should be taken into account in expansion (5). By using (4) and (5), we studied the evolution of the envelope of a femtosecond PBLB taking into account the combined influence of the second- and third-order dispersion effects. The numerical experiment has shown that the propagation velocity of the maximum of the PBLB envelope at small distances behind the axicon [$z \leqslant z_B/3$, where $z_B = w/\tan\gamma(\omega_0)$ is the diffraction-free region] exceed the group velocity [for curve (*1*) in Fig. 2, the envelope maximum is displaced to the left along the abscissa from the point $\tau = 0$ corresponding to the propagation of the maximum with the group velocity]. In this case, the envelope shape remains Gaussian and does not change during PBLB propagation. With distance from the axicon the difference of these velocities decreases to zero [curve (*2*) in Fig. 2] and then the envelope deformation is observed, which is accompanied by the appearance of an additional PBLB (satellite) [curve (*3*) in Fig. 2]. The value of the maximum of the satellite envelope depends on the incident pulse duration: the shorter t_0, the greater the maximum of the satellite intensity (Fig. 3). It follows from numerical calculations that the distance between the maxima of the envelopes of the main and additional PBLBs increases with distance from the axicon.

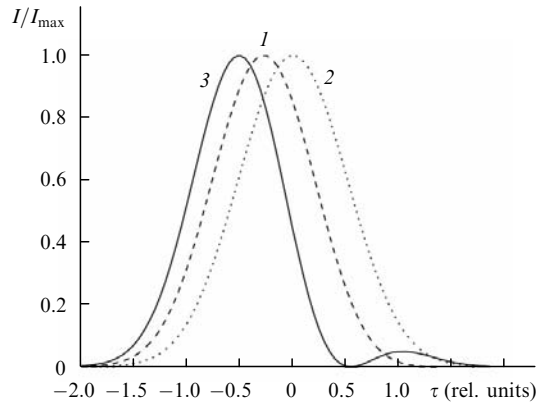

Figure 2. Dependences of the normalised axial beam intensity I/I_{max} on the parameter $\tau = (t - k'_{z,0}z)/t_0$ for the initial pulse duration 70 fs, the axicon base angle 2°, and distances from the axicon 5 (*1*), 10 (*2*), and 15 cm (*3*).

The appearance of the additional PBLB is explained by the presence of the diffraction field formed by the axicon apex. It is known that the ideal axicon has a conic surface characterised by the presence of a singular (conic) point at the apex. Upon numerical simulation of the Gaussian beam diffraction from the axicon by using the Fresnel integral (3), this singularity leads to the appearance of an additional field diffracted from the axicon apex, which can be treated as a spherical wave in the first approximation. The spherical wave is described in the paraxial approximation as a unimodular beam with the Laguerre–Gaussian transverse intensity distribution with the azimuthal index equal to zero. The phase velocity of this beam is smaller than the phase

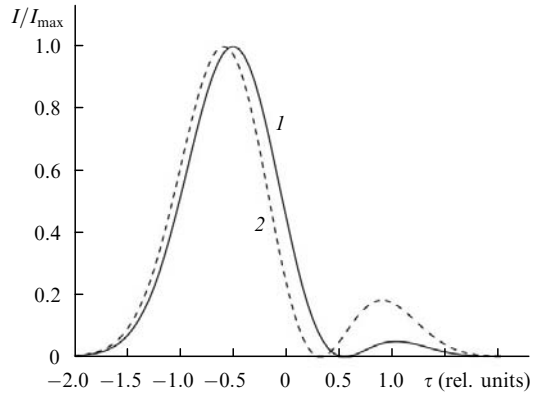

Figure 3. Dependences of the normalised axial beam intensity I/I_{max} on the parameter τ for the distance from the axicon 15 cm, the axicon base angle 2°, and the initial pulse durations 70 (*1*) and 40 fs (*2*).

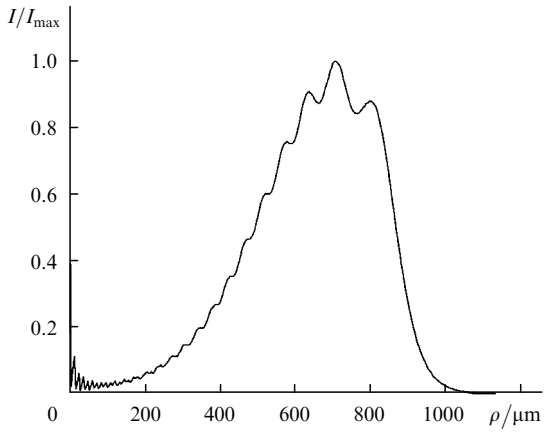

Figure 5. Radial distribution of the normalised radiation intensity I/I_{max} of the 840-nm monochromatic Bessel beam (I_{max} is observed for $\rho = 712$ μm). The beam is formed by the axicon from a Gaussian beam with the beam waist $w = 0.45$ mm; the distance from the axicon is 2.8 cm.

velocity of a monochromatic PBLB of the same frequency. Thus, in the paraxial approximation the light field formed by the axicon illuminated by a Gaussian beam can be represented by a superposition of the Bessel and Laguerre–Gaussian beams propagating at different velocities.

Note that the axicon can be represented in the first approximation by a combination of a truncated conic surface and a spherical (lens-like) surface (Fig. 4). The latter is produced due to a special processing of the axicon during its manufacturing. Thus, the light field observed experimentally upon diffraction of a Gaussian beam from the axicon and obtained in numerical simulation is a superposition of a Bessel light beam (formed by a part of the axicon restricted by the truncated conic surface) and a Laguerre–Gaussian beam with the azimuthal index equal to zero (formed by the effective lens). The formation of such a beam behind the axicon illuminated by a narrow Gaussian light beam is illustrated by numerical calculations (Fig. 5). Figure 5 demonstrates the distinct axial component of the field produced by the axicon in the far-field zone, which is responsible for the formation of a satellite. The appearance of the additional Laguerre–Gaussian beam for each of the frequency components of a Gaussian pulse incident on the axicon leads to the formation of two PBLBs behind the axicon, which propagate with different group velocities. Due to a short duration of the incident pulse and difference in the group velocities of pulsed beams formed by the axicon, they are spatially separated in the longitudinal direction.

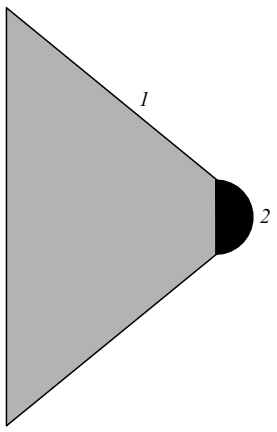

Figure 4. Axicon as a combination of a truncated cone (*1*) and a spherical lens (*2*).

To confirm the above explanation of the predicted effect, we studied the properties of the transformation of pulses with the higher-order Laguerre–Gaussian profiles with the envelope described by the expression

$$E(0,\rho,t) = E_0 \exp\left(-\frac{t^2}{t_0^2}\right) \exp\left(-\frac{\rho^2}{2w^2}\right)\left(\frac{\rho}{\sqrt{2}\,w}\right)^m \times L_n^m\left(\frac{\rho^2}{w^2}\right) \exp(\mathrm{i}m\varphi) \exp(\mathrm{i}\omega_0 t), \quad (8)$$

where $L_n^m(x)$ are Laguerre polynomials and $\exp(\mathrm{i}m\varphi)$ is the phase factor. The distinct feature of the higher-order Laguerre–Gaussian beams ($m \neq 0$) is the minimal intensity on the beam axis, which excludes diffraction effects at the axicon axis. Numerical simulations performed by using (3) and (4) with the replacement

$$\exp\left(-\frac{\rho^2}{2w^2}\right) \to \exp\left(-\frac{\rho^2}{2w^2}\right)\left(\frac{\rho}{\sqrt{2}\,w}\right)^m \times L_n^m\left(\frac{\rho^2}{w^2}\right) \exp(\mathrm{i}m\varphi)$$

in (3) show that in this case one PBLB is formed behind the axicon (Fig. 6). This confirms our explanation of the appearance of the satellite upon incidence of a Gaussian pulse on the axicon.

3. Experimental study of the formation of a femtosecond PBLB by an axicon

Pulsed Bessel light beams were produced by using a setup with a Tsunami (Spectra-Physics) femtosecond Ti : sapphire laser emitting 40-fs pulses with a pulse repetition rate of 85 MHz and an average power of 0.5 mW (Fig. 7). By focusing radiation in an axicon, we obtained ultrashort PBLBs with the transverse intensity distribution presented in Figs 8 and 9. One can see from Fig. 9 that the intensity distribution in the beam cross section can be approximately

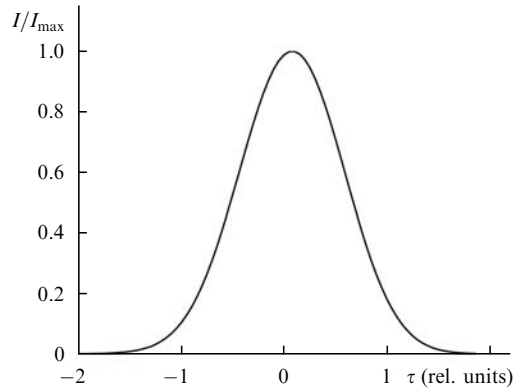

Figure 6. Dependence of the normalised axial beam intensity I/I_{max} on the parameter τ upon illumination of the axicon by a Laguerre–Gaussian pulse with the transverse profile $r\exp(-r^2/2w^2)$. The distance from the axicon is 15 cm, the initial pulse duration is 70 fs, and the axicon base angle is 2°.

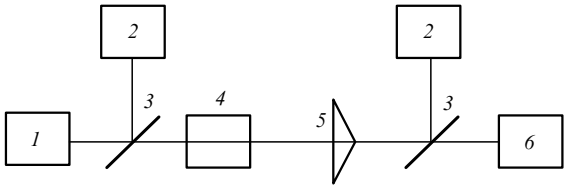

Figure 7. Optyical scheme of the experimental setup for studying the spatial PBLB intensity distribution; (*1*) Tsunami Ti : sapphire laser; (*2*) spectrum analyser; (*3*) beamsplitter; (*4*) telescope; (*5*) axicon; (*6*) CCD camera with a microscope objective.

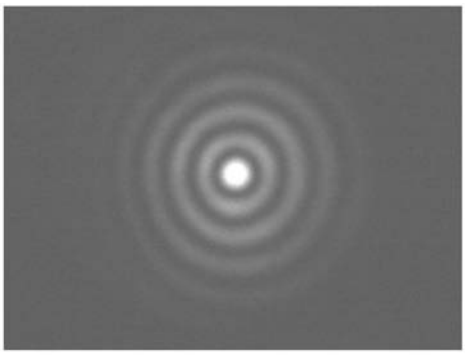

Figure 8. Transverse intensity distribution in a PBLB formed by the axicon.

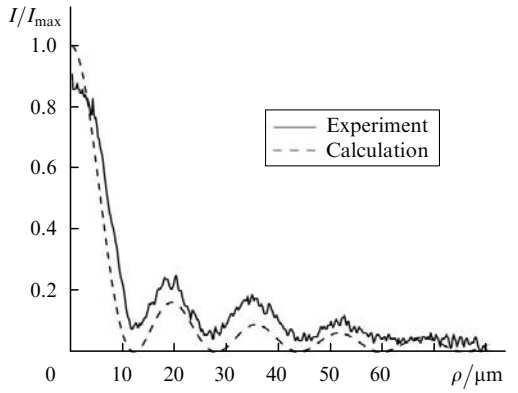

Figure 9. Dependences of the PBLB intensity normalised to its calculated value on the z axis on the radial coordinate ρ.

described by the square of the zero-order Bessel function according to (3) and (7).

In addition, we measured experimentally the PBLB spectrum (Fig. 10). One can see from Fig. 10 that the PBLB spectrum is narrower (approximately by 20 %) than the spectrum of the incident Gaussian pulse.

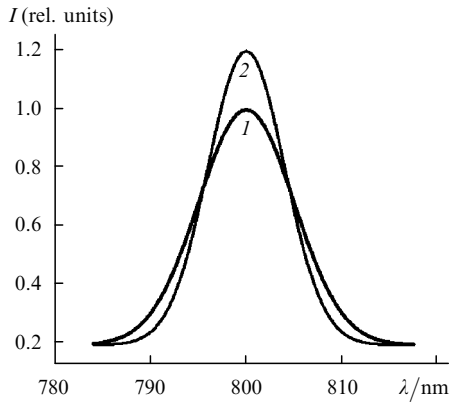

Figure 10. Emission spectra of PBLBs incident on the axicon (*1*) and formed in it (*2*).

We also measured the longitudinal distribution of the light field intensity behind the axicon (Fig. 11) and found that the intensity maximum of the femtosecond PBLB was observed at a distance of 8 cm from the axicon. The beam diameter slightly increased and its intensity slowly decreased with distance from the axicon up to z_B. In this case, unlike monochromatic PBLBs, the boundary of the region in which diffraction effects were absent was diffuse and elongated. In addition, experiments showed that the longitudinal distribution of the femtosecond PBLB intensity was similar to that for a monochromatic Bessel beam, the only difference being that the minimum intensity was nonzero.

Note that, by placing a lens in front the axicon in the optical scheme in Fig. 7, which provides the control of the divergence of the incident Gaussian pulse, we can form PBLBs for which the diameter and maximum intensity of the central maximum change in the longitudinal direction.

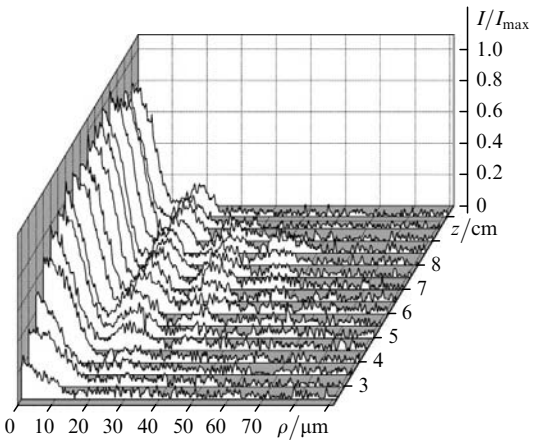

Figure 11. Transverse intensity distribution in the PBLB normalised to its maximum value I_{max} for $z = 8$ cm as a function of the longitudinal coordinate z.

By mounting an aperture in a telescopic system [element (*4*) in Fig. 7], it is possible to control the size of the range of existence of a PBLB formed by the axicon by varying the aperture diameter.

4. Conclusions

We have studied theoretically and experimentally the spatiotemporal dynamics of the PBLB formed by an axicon. The appearance of a satellite, whose maximum intensity depends on the incident pulse duration, has been predicted. It has been shown that the PBLB diameter virtually does not change with distance from the axicon and the PBLB intensity slightly decreases up to the distance z_B; however, the boundary of the diffraction-free region is diffuse and elongated. It has been found that PBLBs with the required parameters (the central maximum diameter and intensity) can be generated from a Gaussian pulse by using an optical scheme containing an axicon and a lens.

Acknowledgements. The authors thank V.N. Belyi and N.A. Khilo for useful discussion of the results obtained in the paper.

References

1. Porras M.A. *Opt. Lett.*, **26**, 1364 (2001).
2. Porras M.A., Borghi R., Santarsiero M. *Opt. Commun.*, **206**, 235 (2002).
3. Hu W., Guo H. *J. Opt. Soc. Am. A*, **19**, 49 (2002).
4. Kurilkina S.N., Belyi V.N., Kazak N.S. *Proc. SPIE Int. Soc. Opt. Eng.*, **6613**, 661303-01 (2007).
5. Durnin J., Miceli J.J., Eberly J.H. *Phys. Rev. Lett.*, **58**, 1499 (1987).
6. McLeod J.H. *J. Opt. Soc. Am. A*, **44**, 592 (1954).
7. Arimoto R., Saloma C., Tanaka T., Kawata S. *Appl. Opt.*, **31**, 6653 (1992).
8. Bin Z., Zhu L. *Appl. Opt.*, **37**, 2563 (1998).
9. Arlt J., Dholakia K. *Opt. Commun.*, **177**, 297 (2000).
10. Lei M., Yao B. *Opt. Commun.*, **239**, 367 (2004).
11. Pu J., Zhang H., Nemoto S., Zhang W. *J. Opt. A: Pure Appl. Opt.*, **1**, 730 (1999).
12. Martirosyan A., Altucci C., de Lisio C., Porzio A., Solimeno S., Tosa V. *J. Opt. Soc. Am. A*, **21**, 770 (2004).
13. Lin J., Wei M., Liang H., Lin K., Hsieh W. *Opt. Express*, **15**, 2940 (2007).
14. Paterson C., Smith R. *Opt. Commun.*, **73**, 448 (1989).
15. Vasara A., Turunen J., Friberg A.T. *J. Opt. Soc. Am. A*, **6**, 1748 (1989).
16. Lee H.S., Steward B.W., Choi K., Fenichel H. *Phys. Rev. A*, **49**, 4922 (1994).
17. Belyi V.N., Kazak N.S., Khilo N.A. *Kvantovaya Elektron.*, **30**, 753 (2000) [*Quantum Electron.*, **30**, 753 (2000)].
18. Khilo N.A., Petrova E.S., Ryzhevich A.A. *Kvantovaya Elektron.*, **31**, 85 (2001) [*Quantum Electron.*, **31**, 85 (2001)].
19. King T.A., Hogervorst W., Kazak N.S., Khilo N.A., Ryzhevich A.A. *Opt. Commun.*, **187**, 407 (2001).
20. Wulle T., Herminghaus S. *Phys. Rev. Lett.*, **70**, 1401 (1993).